

The above equation holds well for  $\phi(\theta, \tau) = \phi(\theta\tau)$ . The kernel of this type is also known as product kernel.

### 2.2.6. Limitations

The unified approach has been presented to construct new distributions with desired properties by varying the properties of the kernel. However, the kernel is not varied in time and frequency dependent fashion and hence the distribution is independent of the signal characteristics and does not reflect the true characteristics because of the inherently associated cross terms in bilinear distributions, and signal dependent kernels have to be investigated.

## 2.3. AFFINE CLASS

The Cohen's class includes all the quadratic distributions that are invariant to shifts in time and frequency. We can define an operator (e.g., shift in time, shift in frequency, shear in frequency, etc.) and construct distributions that are covariant to shifts on these operators. When we choose scale and time shifts as the operators, we obtain the Affine class (O'Neil, 1997). Time-frequency distributions in the Affine class can be computed through smoothening of the Wigner distribution, as WVD is covariant to both shift in frequency and scale. For example, the Affine class can be written as:

$$A(t, \omega) = \iint W(t', \omega') \phi(\omega(t' - t), \omega' / \omega) dt' d\omega'. \quad (2.11)$$

The relationship between the Affine class and the wavelet transform is similar to the relationship between Cohen's class and the short-time Fourier transform. The scalogram is defined as the squared magnitude of the wavelet transform. We can construct

innumerable distributions that fundamentally differ from Cohen's class, but can be constructed using the same general structure by defining a new set of operators on which the class would be covariant. Recently, Papandreou *et al*, have defined another class of quadratic class called "hyperbolic class". This class consists of all quadratic time-frequency distributions that are covariant to hyperbolic shifts in time ( Papandreou *et al*, 1993). The hyperbolic time shift operator is defined as:

$$(H_h)(t) = e^{-jh \log t} x(t). \quad (2.12)$$

More information on the existence and construction of arbitrary operators can be found in (Baraniuk *et al*, 1996). Higher order distributions were proposed to match very specific signals that have nonlinear frequency modulation or polynomial instantaneous frequency, e.g., Wigner-bispectrum, polynomial Wigner distribution and L-Wigner distribution (Stankovic, 1994).

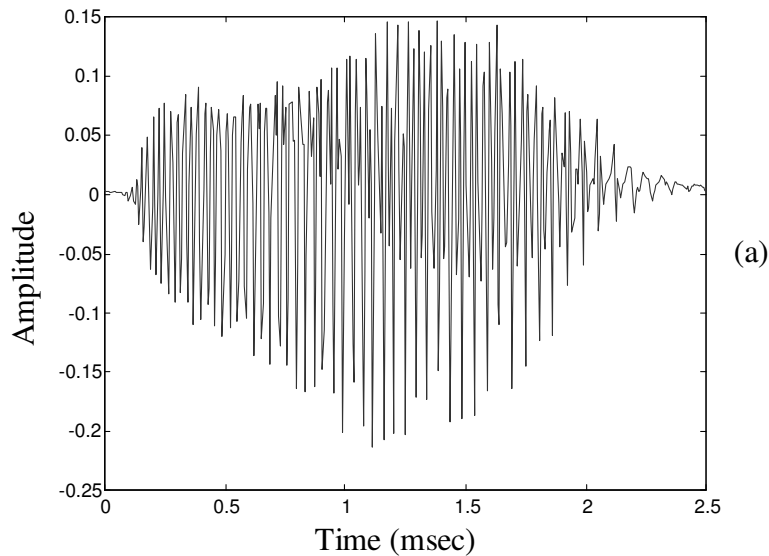
## 2.4. ADAPTIVE TFDs

The TFDs in the Cohen's class can be obtained by convolving the Wigner distribution with the kernel function. As mentioned earlier, the purpose of this kernel is to filter out cross terms and maintain the resolution of the auto terms. Since the structure of the auto terms in the Wigner distribution changes with signals, the kernels that work well for one signal may not work well for other signals. A fixed kernel results in good performance for only certain configurations of ambiguity function auto terms and cross terms. Since the locations of the auto components and cross components depend on the signals to be analyzed, we expect to obtain good performance for a broad class of signals by using only the signal dependent kernel. Jones *et al* have proposed methods for creating signal

adaptive kernels (Jones *et al*, 1993a). The optimal kernel design is formulated in the ambiguity plane because of its property to distinguish the auto components and cross components, and can be formulated as:

$$\max_{\phi} \int_{-\infty}^{\infty} \int_{-\infty}^{\infty} |A(\theta, \tau) \phi(\theta, \tau)|^2 d\theta d\tau,$$

which is subject to the constraints:  $\phi(0,0) = 1$  and  $\phi(\theta, \tau)$  is radially non-increasing. TFD of a bat signal using the adaptive optimal kernel design is shown in Fig. 2.7. A fast algorithm to compute the above representation is proposed in (Jones *et al*, 1994b). Further, constraining the kernel to be a radially Gaussian kernel is proposed in (Jones *et al*, 1993c). Jeong *et al* have investigated the kernel design for reduced interference (Jeong *et al*, 1992a). Jones *et al* have considered the problem of finding a best estimate using short-time Fourier transform (STFT) by choosing a concentration measure and then adapting the window parameter in each time and frequency bin using this measure (Jones *et al*, 1992b). They claim that it outperforms all representations in terms of concentration, but it is computationally very extensive.



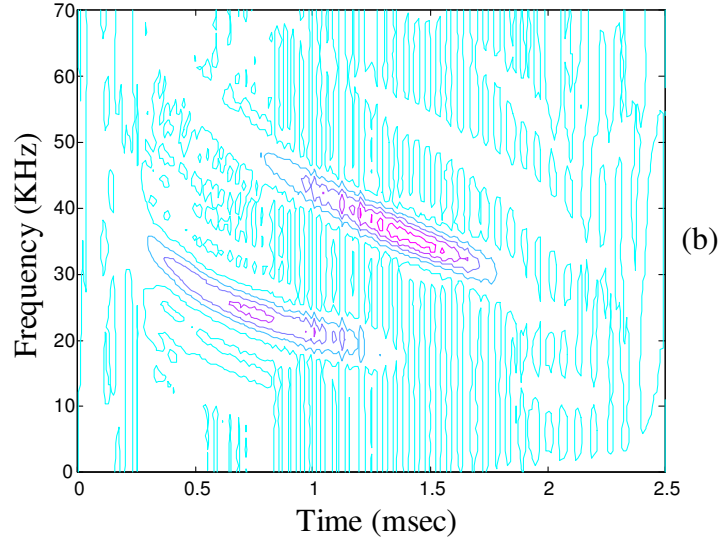


**Fig. 2.7. (a) A bat signal and (b) Adaptive optimal kernel time-frequency representation of the signal**

## 2.5. OTHER REPRESENTATIONS

Flexible decompositions are particularly important for representing signal components whose localizations in time and frequency vary. Hence, a multidimensional parameter space is considered to reveal the signal's inner structure more effectively. Extending the analysis domain beyond time and frequency is gaining momentum. However, the existing methods have their limitations from the computational point of view (Baraniuk *et al*, 1996b). We now review some decomposition algorithms.

### 2.5.1. Matching Pursuits

The matching pursuits algorithm decomposes any signal into a linear expansion of waveforms that are selected from a redundant dictionary of functions (Mallat *et al*, 1993).

These waveforms are chosen in order to match the signal's structures best. These are

general procedures to compute adaptive signal representations. Decompositions of signals over the family of functions that are well localized in time and frequency have found many applications in signal processing. Such functions are called time-frequency atoms. A general family of time-frequency atoms can be generated by scaling, translating and modulating the window signal. In general, we can represent a signal expanded in terms of these atoms, as:

$$f(t) = \sum_{n=-\infty}^{\infty} a_n g_n(t). \quad (2.13)$$

This algorithm finds its expansion set by successive approximations of  $f$  with orthogonal projections on elements of the dictionary. The vector  $f$  can be decomposed into:

$$f = \langle f, g_{\gamma_0} \rangle g_{\gamma_0} + Rf, \quad (2.14)$$

where  $Rf$  is the residue vector after approximating  $f$  in the direction of  $g_{\gamma_0}$ . The above equation is computed iteratively until the residue vector approaches a threshold assuring that the signal can be reconstructed from the expansion set with a tolerable error. Adaptive time-frequency representations can be constructed using these expansion coefficients. Some of its applications in spectral estimation, denoising, multicomponent separation, etc., can be found in (Mallat *et al*, 1993).

### 2.5.2. Atomic Decomposition

Atomic decomposition expands any signal in terms of four parameter time-frequency atoms that are localized in the time-frequency plane. The Gaussian function is chosen as the basic atom because of its minimum area property in the time-frequency plane. The

four-parameter atom is obtained by successive applications of scaling, rotation, time and frequency-shift operators to the Gaussian elements, giving:

$$g_{\beta}(t) \triangleq (\Gamma_{\alpha} g_s)(t-u) e^{jvt}$$

$$\triangleq g_{s,\alpha}(t-u) e^{jvt}, \quad (2.15)$$

where  $\beta \triangleq (s, \alpha, u, v) \in \Omega$  is the index of the atom. The scaled and rotated atom is found as:

$$g_{s,\alpha} = \frac{\sqrt{s} e^c}{\pi^{1/4} (\sin^2 \alpha + s^4 \cos^2 \alpha)^{1/4}} \exp\left(-\frac{s^2 - j(s^4 - 1) \cos \alpha \sin \alpha}{2(\sin^2 \alpha + \cos^2 \alpha)} t^2\right), \quad (2.16)$$

$$\text{where } c = \frac{\pi}{4} - \frac{\arctan(s^2 \cot \alpha)}{2}.$$

The decomposition is done via the matching pursuits in which the dictionary is constituted by the four-parameter space. A similar kind of approach in representing the signal as a sum of chirped Gaussians can be found in (Bultan, 1999). Adjustment of rectangular shell shapes adapted to the local structure will permit a clearer representation of the signal. The oblique cells are obtained by chirping the Gaussian. Its applications in finding the drift rate and separation of multicomponents are also presented.

### 2.5.3. Fractional Fourier Transform

The fractional Fourier transform (FRFT) rotates the time-frequency plane with a specified angle. This can cause the analysis grid to shear in time-frequency plane and can represent signals of dispersive nature. It is defined for any function  $f(t)$ , as:

$$f_{-\alpha}(t) \triangleq (\Gamma_{-\alpha} f)(t) \quad (2.17)$$

$$\triangleq \sqrt{\frac{1-j\cot\alpha}{2\pi}} e^{j\frac{\cot\alpha}{2}t^2} \int f(\tau) e^{j\frac{\cot\alpha}{2}\tau^2} e^{-j\csc\alpha\tau t} d\tau$$

where  $\Gamma$  is the rotation operator corresponding to the counter-clockwise rotation of  $\alpha$  radians. The FRFT is equal to the Fourier transform at  $\pi/2$ . The discretization of FRFT is considered in (Bultan *et al*, 1998). An example depicting the rotation of the time-frequency plane at an angle of  $\pi/2$  is shown in Fig. 2.8.

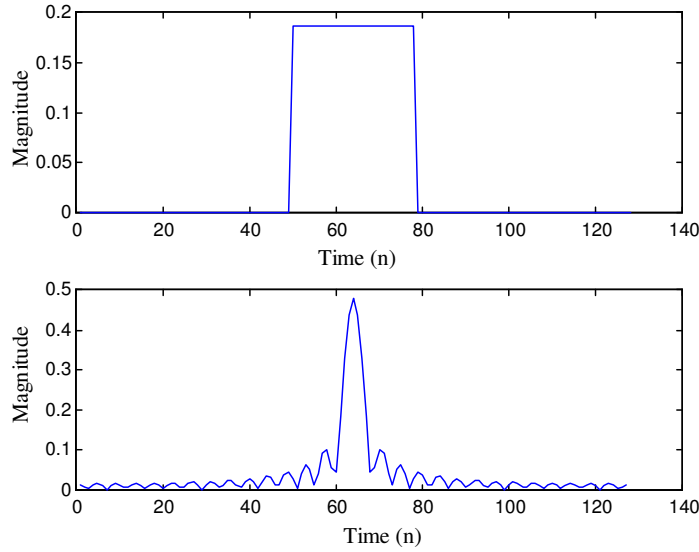


**Fig. 2.8. (a) A rectangular pulse and (b) It's Fractional Fourier transform at  $\alpha=\pi/2$**

#### 2.5.4. Short-Time Fourier Transform

The STFT analysis and synthesis are fundamental for describing any quasi-stationary signals such as speech. As mentioned in our earlier discussion, the Fourier transform does not explicitly show the time localization of the frequency components. So the time

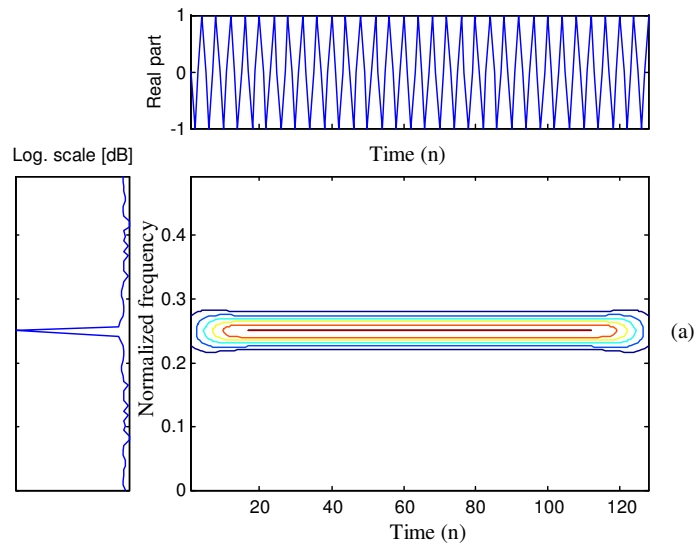
localization can be obtained by suitably pre-windowing the signal  $s(t)$  (Nawab *et al*, 1988). The STFT can be defined as :

$$S_x(u, \zeta) = \langle x, g_{u, \zeta} \rangle = \int x(t) g(t - u) e^{-j\zeta u} dt . \quad (2.18)$$

It uses an atom which is the product of a sinusoidal wave with a symmetric finite energy window function  $g$ . These atoms are obtained by time translations and frequency modulations of the original window function:

$$g_{u, \zeta}(t) = g(t - u) e^{j\zeta t} . \quad (2.19)$$

The atom is time centered at  $\tau$  and frequency centered at  $\zeta$ . Multiplication by a relatively short window effectively suppresses the signal outside the neighborhood around the “analysis time”  $u$ . The effect of varying the length of the window is shown in Fig. 2.9.





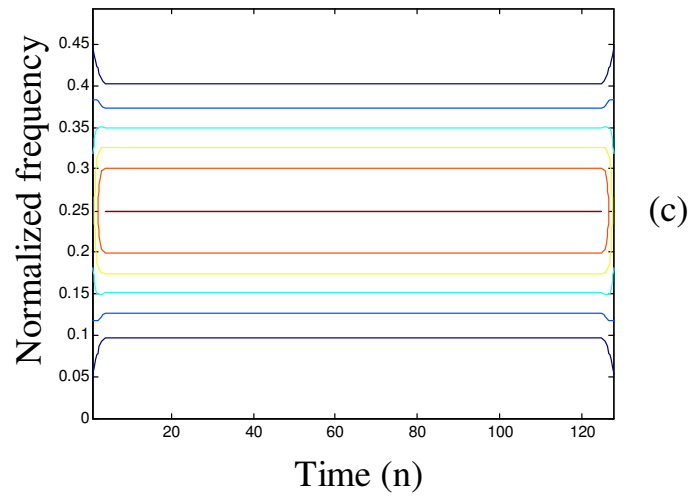
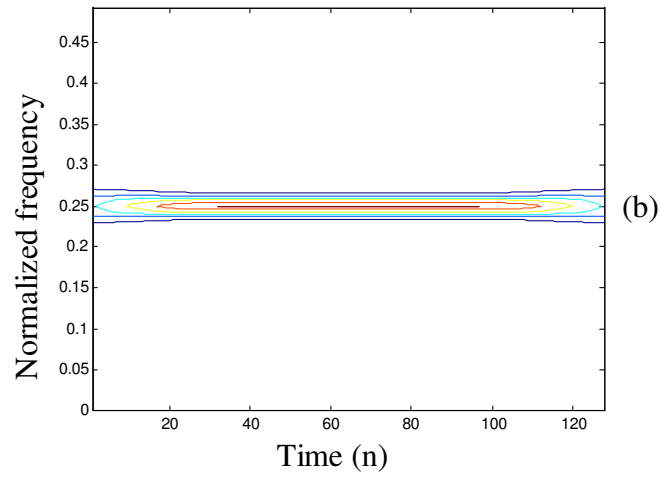


**Fig. 2.9.** (a) Energy spectral density, real part and STFT of a 128 point truncated sinusoid, (b) STFT with 64 point Hamming window and (c) STFT with 7 point Hamming window

The localization and energy concentration of STFT depends only on the window and does not vary unless the window is changed, i.e., the time and frequency spread are

constant throughout. This can be considered as a bank of filters having constant bandwidth as exemplified in Fig. 2.10.

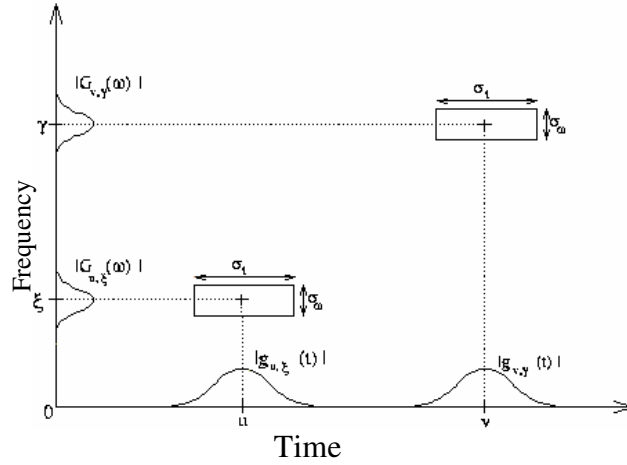


**Fig. 2.10. Time-frequency tilings in STFT analysis**

### 2.5.5. Wavelet Transform

The wavelet transform (WT) provides an alternative to the classical STFT or Gabor transform for the analysis of nonstationary signals. It also provides a unified framework for a number of techniques such as multiresolution analysis, subband coding, and wavelet series expansions that have been developed for various signal processing applications. In contrast to the STFT, the WT uses short windows at high frequencies and long windows at low frequencies. The continuous wavelet transform can be defined as:

$$WT_x(u, s) = \langle x, \psi_{u,s} \rangle = \int_{-\infty}^{\infty} x(t) \frac{1}{\sqrt{s}} \psi^* \left( \frac{t-u}{s} \right) dt, \quad (2.20)$$

where the mother wavelet  $\psi$  is a zero-averaging function centered around zero with finite energy. The *db4* mother wavelet and the scaling function are shown in Fig. 2.11. The atoms are obtained by translations and dilations of the mother wavelet as:

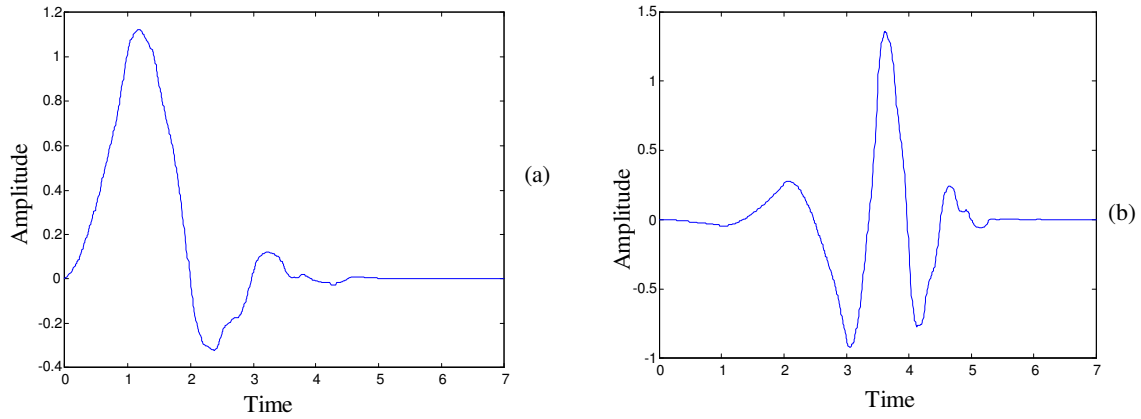


**Fig. 2.11. (a) The *db4* scaling function and (b) The *db4* mother wavelet**

$\psi_{u,s}(t) = \frac{1}{\sqrt{s}} \psi\left(\frac{t-u}{s}\right)$  that is centered around  $u$ . If the frequency centering of  $\psi$  is

$\eta$ , then the frequency centering of the dilated function is  $\eta / s$ . The time spread of the above function is proportional to  $s$  and the frequency spread is inversely proportional to  $s$ . It is as though the filters have a constant  $Q$ , bandwidth being proportional to the frequency. The time-frequency support of the WT is shown in Fig. 2.12. The WT applied to a narrow rectangular pulse demonstrates the time localization properties shown in Fig. 2.13. It can be observed from the figure that at lower scales or in high frequency regions, the WT is localized in time. However, at higher scales the frequency resolution is better. Wavelet analysis is capable of revealing aspects of data that other signal analysis techniques miss, for example aspects like trends, breakdown points, discontinuities in

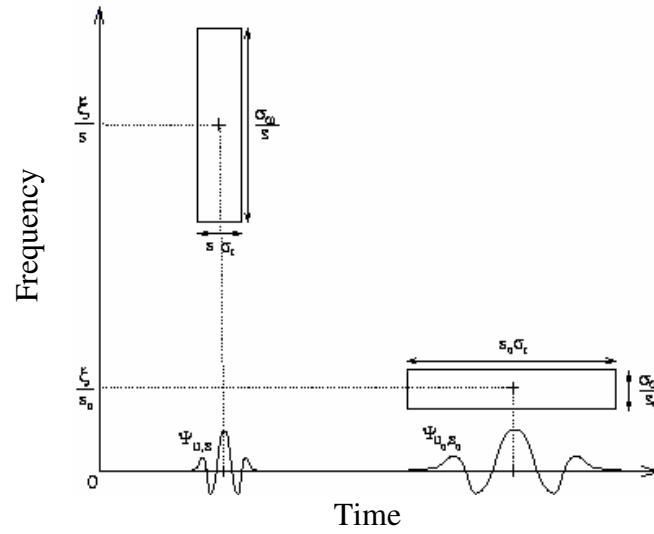


**Fig. 2.12. Time-frequency tilings in the wavelet analysis**

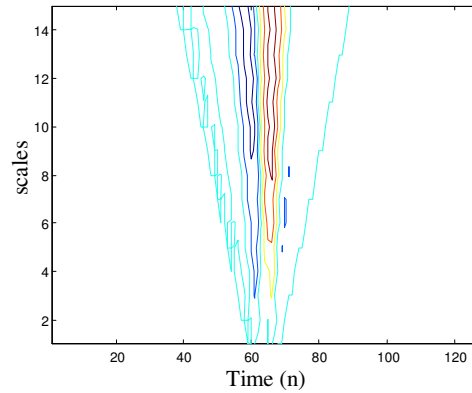


**Fig. 2.13. Wavelet tranform of a narrow rectangular pulse using *db4* wavelet**

higher derivatives and self-similarity. Further, because it affords a different view of data than those presented by traditional techniques, wavelet analysis can often compress or de-noise a signal without appreciable degradation. A good review on wavelet transform, its applications, the filter bank interpretation and fast computations can be found in (Rao *et al*, 1998).